Deformation behavior of AA6061 with 5% by volume Al_2O_3 under hot deformation condition

[1]Madhur Chandra Dixit, [2]Tushar Pandey, [3]Avtansh Dixit

[1]HVAC Engineer, [2]System Engineer, [3]Student
[1]AWACPTS Lucknow, [2]Siemens-Energy, [3]Department of Plastic Technology (HBTU Kanpur)

***Abstract*- The hot deformation behavior and constitutive relationship of AA 6061 aluminum alloy with 5% by volume Al_2O_3 was studied after carrying out hot isothermal compression tests using Gleeble 3800® thermo-mechanical simulator, range of temperature and strain rate was 573˚K to 773˚K and 0.001 to 1 s^{-1}, respectively and the height reduction was of 70%. One of the important features observed in the material is Dynamic Strain Aging, which was observed from temperature ranging from 573˚K to 673˚K at strain rate of .001, .01, .1, 1 s^{-1}. The modified Arrhenius type constitutive equation models based on Zener-Holloman parameter were used. The power law and sine-hyperbolic law were used to calculate activation energy. The value of activation energy using sine-hyperbolic law comes out to be 212.205 kj/mol. The value of activation energy was found to be much higher than self diffusion activation energy of pure aluminum alloy (144 kj/mol). The high value of activation energy suggests that DRV or DRX can be a leading softening mechanism.**

***Keywords*: Hot Deformation, AA6061, Activation Energy, Softening Mechanism**

1. INTRODUCTION

Hot deformation behaviour of materials is dependent on various processing parameters like hydrostatic pressure, temperature, strain rate, time, and strain. In engineering calculations strain rate, strain and temperature are considered only [1]. To relate these variables constitutive models such as Zerilli and Armstrong model, Johnson-Cook model, Arrhenius model are used. These models provide complete mathematical description of the flow stress of material [2]. The phenomenon like work hardening (WH), dynamic recovery (DRV), and dynamic recrystallization (DRX) affects the deformation mechanism of materials which makes mechanism of materials flow behavior under hot deformation condition is quite complex in nature [3]. Another important phenomenon known as dynamic strain aging (DSA) occur under certain temperature and strain rate in some material and alloys. In most of the material DSA improves the tensile and fatigue strength, while DSA pre treatment can improve the creep strength of material [4, 5]. Serajzadeh et al. [6] discussed the flow behavior of AA2017–10% SiCp under uniaxial compression test. The activation energy comes out to be 303 kJ/mole, which is greater than the energy required for bulk diffusion of substitutional atoms in Al alloys. At temperature lower than 250˚C, at higher strain (0.3) negative strain rate sensitivity was detected which is discussed by the effect of dynamic strain aging and flow localization was also find to be possible. Fan et al. [7] studied hot deformation behavior of Armco-type pure iron under isothermal compression test. The modified sine-hyperbolic constitutive equation was used for constitutive modeling of material; co-relation coefficient value for experimental and predicted value comes out to be 0.9954; under α-Fe co-relation coefficient value is 0.9711. Bo Li et al. [8] conducted hot compression test on Al-Zn-Mg alloy containing small amount of Sc and Zr With increasing strain rate and decreasing deformation temperature, the flow stress increases. The main dynamic softening mechanism was caused by dynamic recovery and dynamic recrystallization.

Due to high strength to weight ratio, corrosion resistance, toughness, machinability, AA 6061 is widely used [9-11]. It is an important construction material for manufacturing automobiles and aircraft parts. Many studies have been proposed by authors to describe the mechanical and microstructural behavior of AA6061. Dorbane et al. [12] carried out uniaxial tensile test on a rolled AA6061-T6 alloy at different temperatures (25, 100, 200, 300˚C) and strain rates (10^{-4}, 10^{-3}, $10^{-2}$and $10^{-1}s^{-1}$). Microstructural observations showed the elongation of grains in the loading direction. Between room temperature and 200˚C, activation energy equals 52.7 kJ/mol whereas between 200˚C to 300˚C the activation energy was calculated 365 kJ/mol, which have been found comparable to activation energy for creep [13].

Jafarlou et al. [14] performed equal channel angular processing process (ECAP) to produce ultra fine grain structure of AA6061. Finite Element Analysis (FEA) was carried out to check the feasibility of proposed method and deformation mechanism. The significant increase in yield strength, ultimate strength under shear for tubular AA 6061 has been reported. But ductility was found to be decreased for ECAP-processed alloy. Khamei et al. [15] discussed that hot tensile test results showed shifting of super plasticity to higher strain rates with increase in temperature. Recovery of dislocations was reported to be the dominant deformation mechanism. Odeshi et al. [16] compare the performance of AA6061-T6 composite with 10% and 20% alumina by volume under hot torsion test and hot compression test at high strain rates. The deformation was characterized by extensive adiabatic heating and thermal softening of the materials which dominates over strain hardening effect. Xia et al. [17] Carried out hot torsion test on particle reinforced AA6061 with 10 vol% Al_2O_3. The composite shows higher hardening behavior from room temperature to 200˚C due to high dislocation density. From room temperature to 200˚C the activation energy was 36 kj/mol and from 200 to 500˚C the activation energy was 213 kj/mol. High difference in values of activation energy implies different softening mechanism. The softening mechanism at high temperature was considered climb which was cross-slip at low temperature.

2. MATERIAL AND EXPERIMENTAL SETUP

Table 1. The chemical composition of AA 6061

Component	Al	Mg	Si	Fe	Cu	Zn	Ti	Mn	Cr
Amount	97.591	0.88	0.70	0.18	0.29	0.003	0.02	0.33	0.006

The material also contains 5% by volume Al_2O_3. The hot compression test was performed using computer-controlled, servo-hydraulic Gleeble 3800® thermo-mechanical simulator on cylindrical specimen of diameter 10 mm and height 12 mm. The chemical composition of alloy is given in Table 1. The deformation temperatures were 573˚K, 623˚K, 673˚K, 723˚K and 773˚K and strain rates were of 0.001 s^{-1}, 0.01 s^{-1}, 0.1 s^{-1} and 1 s^{-1}. A K-type thermocouple was spot welded at the centre of the specimen to control the temperature during the test on each sample. A graphite foil and a nickel-based lubricant were used between the sample and the ISO-T anvil for the reduction of friction and minimization of temperature gradient, specimens were heated with the heating rate of 5˚Cs^{-1} and held for 3 min to obtain uniform heating. The total true strain of 0.7 was applied and in-situ water quenching was performed.

3. RESULTS AND DISCUSSION

Fig.1 shows the microstructure of the received sample. The microstructure reveals the presence of Al_2O_3. Most of the Al_2O_3 is present near the grain boundaries. Fig.2 shows flow stress vs. strain curves at different temperatures in strain rates ranging from 0.001 s^{-1}, 0.01 s^{-1}, 0.1 s^{-1} and 1 s^{-1}. Curves show that the flow stress behavior of alloy is highly dependent on strain rate and temperature. The flow stress curves at each strain rate consist of a peak value at some

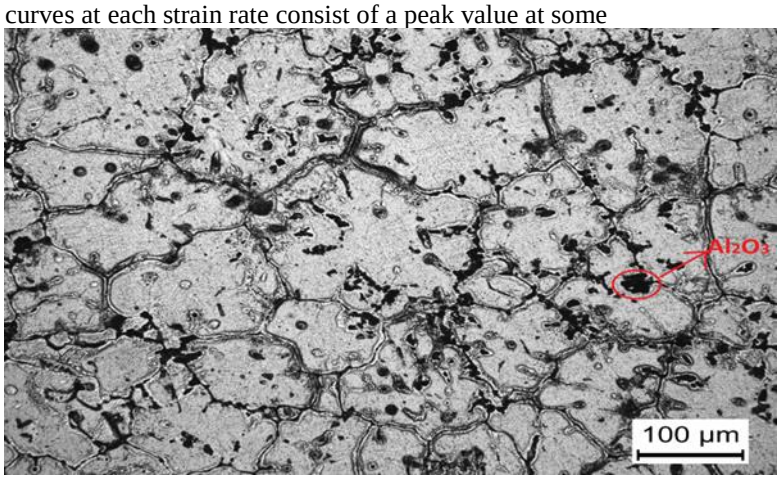

Fig. 1. Microstructure of the examined material (as received) with 5% Al_2O_3

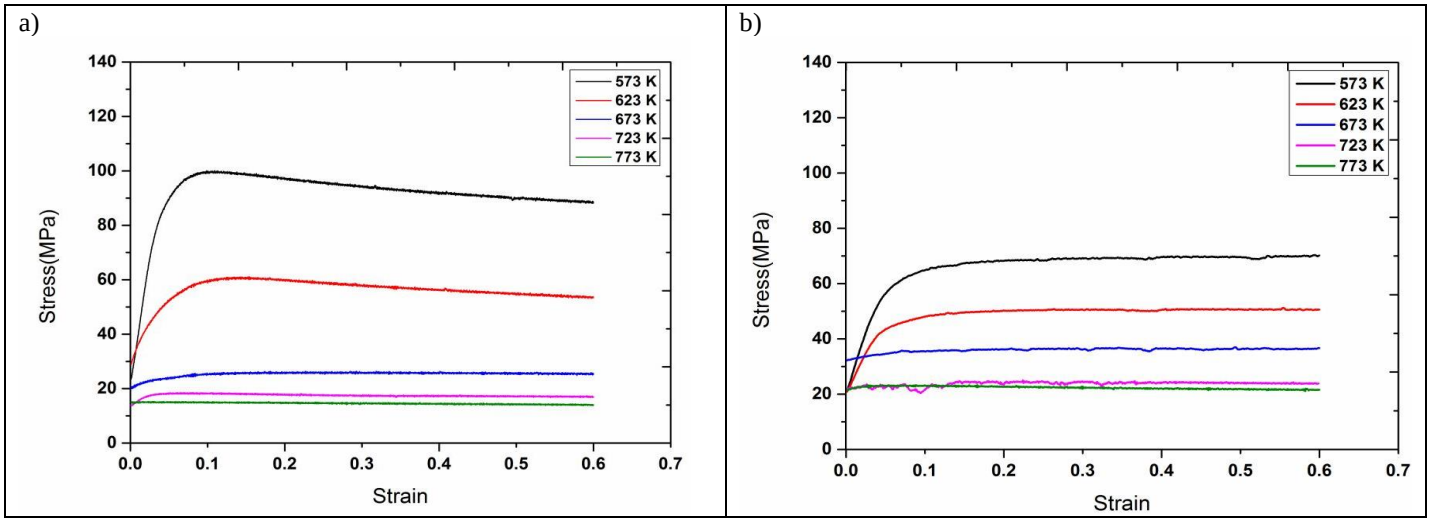

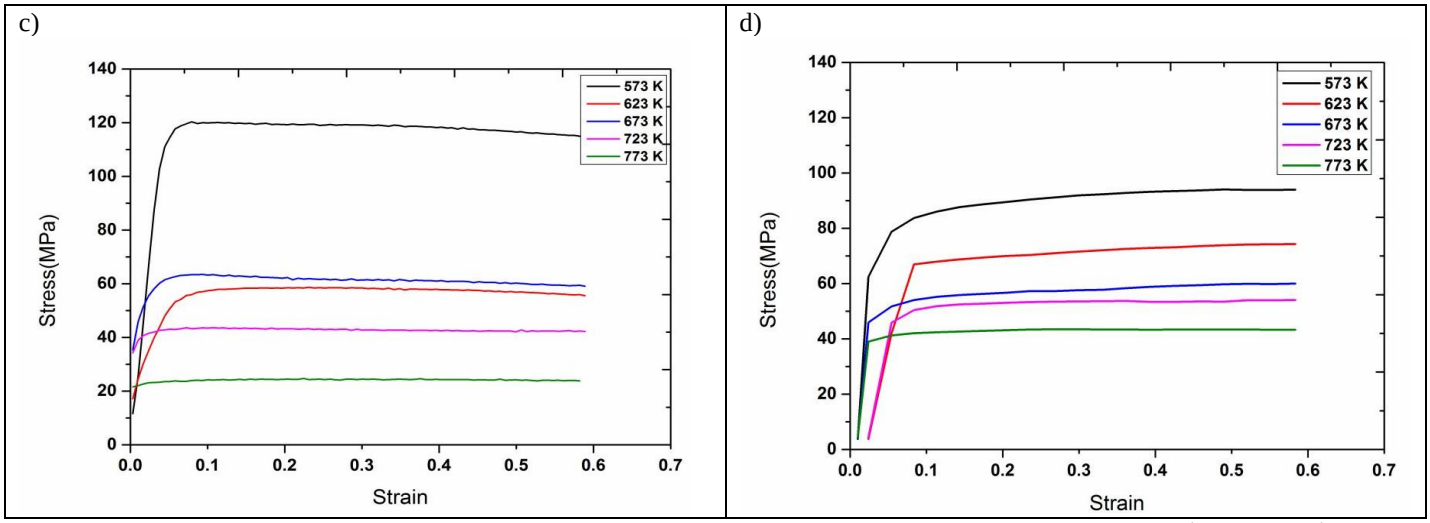

Fig.2 flow stress–strain curves of AA6061 alloy under the different temperatures with strain rates (a) 0.001 s^{-1}, (b) 0.01 s^{-1}, (c) 0.1 s^{-1}& (d) 1 s^{-1}.

low strain level followed by a steady flow region at higher strain values. At initial stage the stress increases to a peak value due to work hardening. But at higher temperature values peak values are not clear. With increase in temperature work hardening in alloy decreases. As shown in fig.1 at any particular strain rate, with increase in temperature the value of peak stress decreases due to growth of work hardening.

The deformation mechanism can be more deeply understood by calculating activation energy using constitutive equations proposed by Sellars and Tegart [19]. During hot deformation of aluminium-based alloy, it has been well accepted that the peak stress can be related to strain rate and deformation temperature through Arrhenius equations. The effects of strain rate and temperature on deformation behaviour can be represented by Zener–Hollomon parameter (Z) in an exponent type equation.

$$Z = \dot{\varepsilon} \exp(\frac{Q}{RT}) \quad \text{....(2)}$$

Where $\dot{\varepsilon}$ is the strain rate, Q is activation energy of hot compression process (J mol^{-1}), R is the gas constant (8.31 J mol^{-1} K^{-1}), T is the absolute temperature (K). The activation energy has been calculated at 0.6 strain. Deformation mechanisms can be deeply investigated by calculating activation energy. According to the different hot deformation conditions, the Zener–Hollomon parameter Z can be expressed as follows [20]:

$$Z = f(\sigma) = A_1 \sigma^{n_1} \quad \text{....(3)}$$

$$Z = f(\sigma) = A_2 \exp(\beta\sigma) \quad \text{....(4)}$$

$$Z = f(\sigma) = A[\sinh(\alpha\sigma)]^n \quad \text{...(5)}$$

Where A, A_1, A_2, n, n_1, β and α are the material constants. Here α is a stress multiplier and can be defined as $\alpha = \beta/n_1$. Eq. (3) is preferred for low strain level ασ< .8 and Eq. (4) is for high strain level ασ> 1.2. Whereas Eq. 4 proposed by Sellars and Tegart is universally accepted over a wide range of stresses [19]. Taking natural logarithm of Eq. (1,2),

$$\ln Z = \ln \dot{\varepsilon} + \frac{Q}{RT} = \ln A_1 + n_1 \ln \sigma \quad \text{....(6)}$$

Eq. 5 can be rewritten as following Eq. 7 and 8

$$\ln \sigma = \frac{1}{n_1} \ln \dot{\varepsilon} + \frac{1}{n_1}(\frac{Q}{RT} - \ln A_1) \quad \text{....(7)}$$

$$\ln \sigma = \frac{1}{n_1}(\ln \dot{\varepsilon} - \ln A_1) + \frac{Q}{n_1 RT} \quad \text{....(8)}$$

Eq. 7 and 8 are the type of y = kx + C. Values of n_1 can be calculated by plotting lnσ vs ln$\dot{\varepsilon}$ at constant temperatures as per Eq. 6 shown in Fig. 3 (a). The value of stress exponent n_1 for power law comes out to be 8.78. Plotting lnσ vs 1/T at constant strain rates as for Eq. 8 gives slope $\frac{Q}{n_1 RT}$ as shown in Fig.3 (b). Using value of n_1, value of activation energy can be calculated which comes out to be 236.37 KJ/mol.

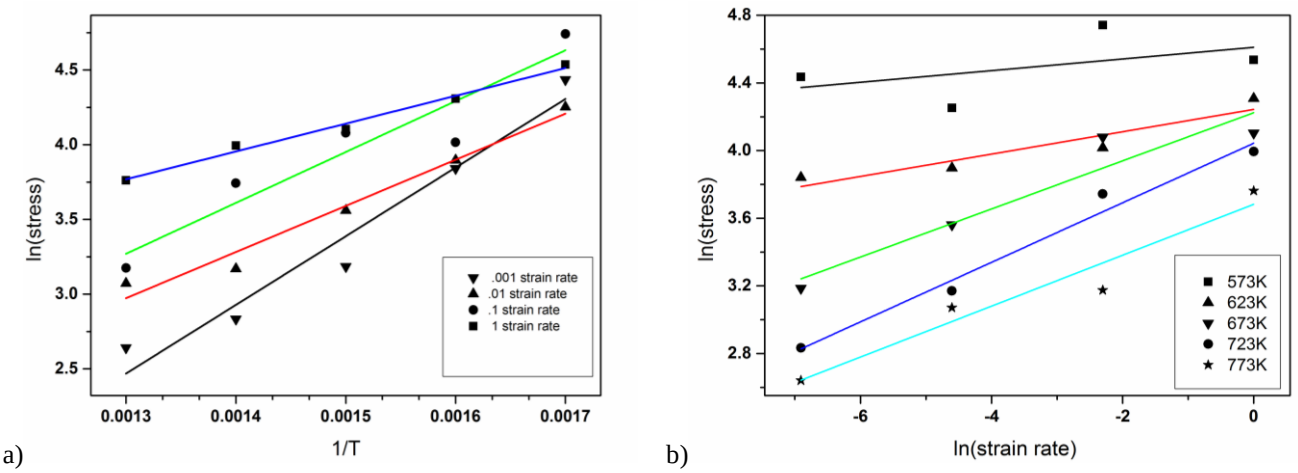

Fig. 3 Relationships between a) lnσ and 1/T, b) lnσ and ln $\dot{\varepsilon}$

As reference to sine hyperbolic law, taking natural logarithm of Eq.1 and 4 we get Eq. 10. Differential equations [13-14] are used to calculate the activation energy. Value of stress multiplier α is taken as 0.052 [20].

$$\ln Z = ln\dot{\varepsilon} + \frac{Q}{RT} = \ln A + n\ln[\sinh(\alpha\sigma)] \quad \text{....(10)}$$

$$n = \frac{\partial \ln \dot{\varepsilon}}{\partial \ln[\sinh(\alpha\sigma)]} \quad \text{....(11)}$$

$$Q = nR\frac{\partial \ln[\sinh(\alpha\sigma)]}{\partial(\frac{1}{T})} \quad \text{.....(12)}$$

Fig. 4 (a) shows the plots of ln $\dot{\varepsilon}$ vs ln[sinh(ασ)] and fig. 4 (b) shows ln[sinh(ασ)] vs 1/T, slopes of these plots are represented in Eq. 9,10. Here the value of n and Q comes out to be 3.10726 and 212.21 KJ/mol.

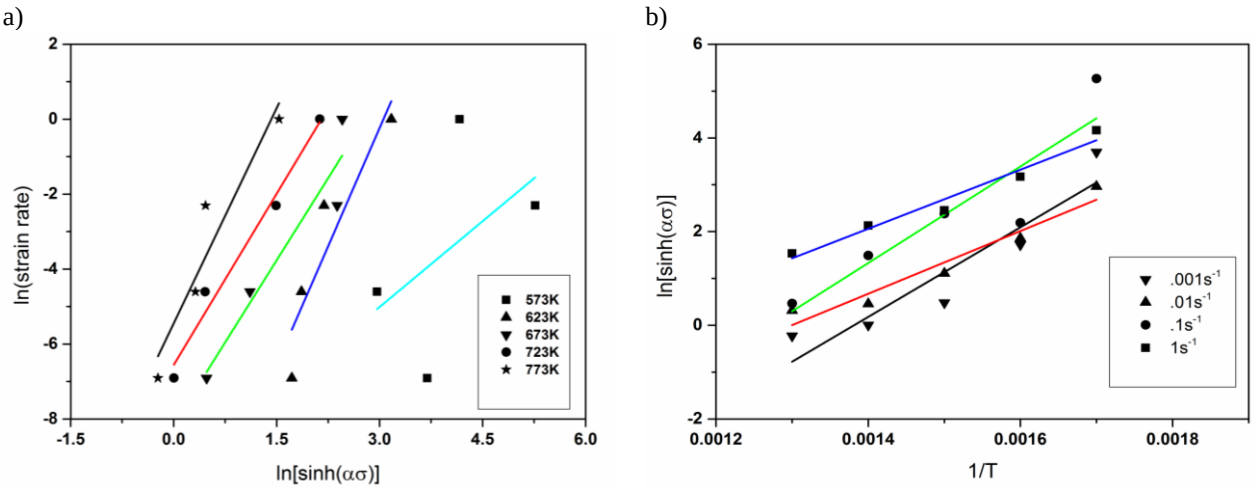

Fig. 4 Relationships between a) ln$\dot{\varepsilon}$ and lnsinh(ασ), b) lnsinh(ασ) and 1/T

The mean activation energy value of the deformed AA6061 (212.21 kJ/mol) is higher than that of the self-diffusion of aluminum (144 kJ/mol) [15-17]. The activation energy is also found to be higher than the energy required for bulk diffusion of substitutional atoms in aluminum alloys [17, 22-23]. The activation energy is also higher than the grain boundary diffusion energy (84 kJ/mol) [24] and that needed for the bulk diffusion of Si or Mg atoms in the matrix which are 136 kJ/mol and 130 kJ/mol [6]. This shows that occurrence of Al_2O_3 may be leading to dynamic restoration process. The activation energy for AA6061 was reported to be 196 kJ/mol [15], which is somewhat lower than for this material. This could be due to the hampering action of the hardening particles on cross slip of mobile dislocation [6, 17]. In such a case, the occurrence of DRV or DRX can lead to high values of Q. L. Shi et al. deduced that the higher Q value of the alloy may be associated with an increase in the Si and Mg held in solution by the homogenization sequence [25].

4. CONCLUSION

The flow behavior of AA6061 with 5% by vol. Al_2O_3 was studied under hot deformation condition for uni-axial compression test, temperature ranging from 573 to 773˚K at constant strain rates of 0.001 s^{-1}, 0.01 s^{-1}, 0.1 s^{-1} and 1 s^{-1}.The experimental results shows that dynamic strain aging occurring in the material which may for the temperature ranging from 573 to 673˚K at strain rate of all four strain rates. Dynamic recovery is the main softening mechanism. At strain rate of .001 s^{-1} the main softening mechanism may be dynamic recovery but at higher temperatures and strain rate the main softening mechanism is dynamic recrystallization. The hot deformation activation energy was calculated to be about 212.21 Kj/mol using sine-hyperbolic law, which is very higher than self diffusion activation energy of pure aluminum.

REFERENCES:

1. An HE, Xi-tao WANG, Gan-lin XIE, Xiao-ya YANG, Hai-long ZHANG, Journal of Iron and Steel Research 22(8) (2015) 721- 729
2. Hong-Ying Li, Ji-Dong Hu, Dong-Dong Wei, Xiao-Feng Wang, Yang-Hua Li, Materials and Design 42 (2012) 192–197
3. Y.C. Lin, Yi Ding, Ming-Song Chen, Jiao Deng, Materials and Design 52 (2013) 118–127
4. Kaiping P, Kuangwu Q, Wenzhe C. Effect of dynamic strain aging on high temperature properties of austenitic stainless steel. Mater Sci Eng A 2004;379:372–7.E.S. Puchi Cabrera, Mater. Sci. Tech. 17 (2001) 155.
5. S. Serajzadeh, S. Ranjbar Motlagh, S.M.H. Mirbagheri, J.M. Akhgar, Materials and Design 67 (2015) 318–323
6. Q.C. Fan, X.Q. Jiang, Z.H. Zhou, W. Ji, H.Q. Cao, Materials and Design 65 (2015) 193–203
7. Bo Li, Qinglin Pan, Zhimin Yin, Materials Science & Engineering A 614 (2014) 199–206
8. D. Maisonnette, M. Suery, D. Nelias, P. Chaudet, T. Epicier, Materials Science and Engineering A 528 (2011), 2718–2724
9. A.O. Adesola, A.G. Odeshi, U.D. Lanke, Materials and Design 45 (2013), 212–221
10. Manas Ranjan Panda, Siba Sankar Mahapatraand Chinmaya,P. Mohanty, Procedia Materials Science 2 2015,2399 – 2406
11. A.Dorbane, G.Ayoub, B.Mansoor, R.Hamade, G.Kridli, A.Imad, Materials Science & Engineering A 624 (2015) 239–249
12. M.A. Meyers, K.K. Chawla, Mechanical Behavior of Materials second edition 2009
13. D.M. Jafarlou, E. Zalnezhad, M.A. Hassan, M.A. Ezazi, N.A.Mardi, A.M.S. Hamouda, M. Hamdi, G.H. Yoon, Materials and Design 90 (2016) 1124–1135
14. A.A. Khamei, K. Dehghani, R. Mahmudi , JOM, Vol. 67, No. 5, 2015
15. A.G. Odeshi, G.M. Owolabi, M.N.K. Singh, and M.N. Bassim, Metall Mater Trans A 2007;38:2674–80
16. Xia X, McQueen HJ, Sakaris P. Hot deformation mechanisms in a 10 vol% Al2O3 particle reinforced 6061 Al matrix composite. Scr Metall Mater 1995;32:1185–90
17. Ko BC, Park GS, Yoo YC. The effects of SiC particle volume fraction on the microstructure and hot workability of SiCp/AA 2024 composites. J Mater Process Technol 1999;95:210–5.
18. Sellars CM, Tegart WM., On the mechanism of hot deformation. Acta Metall, 1966; 14:1136–8.
19. Zerilli FJ, Armstrong RW. Dislocation-mechanics-based constitutive relations
20. for material dynamics calculation. J Appl Phys 1987;61:1816–25.
21. H.J. Mcqueen, Metallurgical and Materials Transaction Vol. 33A 345-362 (2002)
22. P. Sakaris and H.J. McQueen, “Comparative Hot Workability of SiCp/A356 and SiCp/6061 Al Composites and Their Matrices”, Advances in Production and Fabrication of Light Metals, pp. 605-617, ed. by M.M. Avedesian, et al., pub. by CIM Montreal, 1992.
23. A. K. Mukherjee, “High Temperature Creep-Plastic Deformation of Materials”, Treatise on Materials Science and Technology, Vo1.6., ed. by R.J. Arsenault, Academic Press, New York, 1975.
24. E.A. Brandes and G.B. Brook, Smithells Metals Reference Book, 7th ed. (New York: Elsevier, 1992)
25. L. Shi, H. Yang, L.G. Guo, J. Zhang, Materials and Design 54 (2014) 576–581